Metastable phases of 2D boron sheets on Ag(111)

2017 J. Phys.: Condens. Matter 29 095002

(http://iopscience.iop.org/0953-8984/29/9/095002)

IOP Publishing Journal of Physics: Condensed Matter
J. Phys.: Condens. Matter **29** (2017) 095002 (5pp) doi:10.1088/1361-648X/aa5165

Metastable phases of 2D boron sheets on Ag(1 1 1)

Qing Zhong[1], Jin Zhang[1], Peng Cheng[1,2], Baojie Feng[1], Wenbin Li[1], Shaoxiang Sheng[1], Hui Li[1], Sheng Meng[1,2], Lan Chen[1,2] and Kehui Wu[1,2,3]

[1] Institute of Physics, Chinese Academy of Sciences, Beijing 100190, People's Republic of China
[2] University of Chinese Academy of Sciences, Beijing 100049, People's Republic of China
[3] Collaborative Innovation Center of Quantum Matter, Beijing 100871, People's Republic of China

E-mail: lchen@iphy.ac.cn and khwu@iphy.ac.cn

Received 25 October 2016, revised 29 November 2016
Accepted for publication 2 December 2016
Published 27 January 2017

Abstract

Two reproducible new phases of 2D boron sheets have been found on Ag(1 1 1). One of them shares the identical atomic structure of the previously reported S1 phase (β_{12} sheet) but has a different rotational relationship with the substrate, and thus exhibits very different features in scanning tunneling microscopy (STM) images. The other new phase has a hexagonal symmetry and is proposed to be the long-expected α-sheet. Both of these two boron sheets are confirmed to be metallic by scanning tunneling spectroscopy.

Keywords: boron, 2D materials, scanning tunneling microscopy, molecular beam epitaxy, Ag(1 1 1)

(Some figures may appear in colour only in the online journal)

Boron is the fifth element in the periodic table of elements, just before carbon. With only one less valence electron than carbon, boron possesses fairly similar properties to carbon, such as a short covalent radius and the flexibility to adopt sp^2 hybridization, favoring the formation of 2D allotropes [1–3]. Much effort has been devoted to seeking boron nanostructures, such as fullerenes and nanotubes [4–10]. On the other hand, the possibility of the formation of true 2D boron sheets has been seriously considered by theoretical researchers [11–15], since it could be regarded as the structural component of boron fullerenes and nanotubes, just as for carbon structures in graphene [16, 17]. Recently, an experimental breakthrough was made when two parallel works both announced the successful growth of monolayer boron sheets on Ag(1 1 1) by molecular beam epitaxy (MBE) [18, 19]. The successful realization of 2D boron has stimulated the research of nanoelectronics based on boron. Though 2D boron cannot be as stable as graphene and exfoliated from the substrate, the nanodevices may be realized by the growth-transfer-fabrication process similar to silicene [20] or by directly growing 2D boron on a dielectric substrate.

Different to the honeycomb structure of graphene, 2D boron sheets commonly consist of triangular grids with periodic holes due to the electron deficiency of boron [11]. By carving different patterns of hexagonal holes in the triangular boron grids, numerous structures of boron sheets could be constructed [11, 21–23], of which the α-sheet was proposed as the most stable one for free standing 2D boron sheets. However, experimentally, only the β_{12}-sheet and χ_3-sheet have been reported on a Ag(1 1 1) surface by Feng *et al*, corresponding to the S1 and S2 phases they observed, respectively [19]. On the other hand, Mannix *et al* observed an χ_3-sheet and another stripe phase that was at first proposed to be a buckled triangle lattice [18], and then recently confirmed to be a β_{12}-sheet on a reconstructed surface [24]. Note that the energy difference among many theoretical models is very small, and it is thus expected that one should have the chance to observe a significant amount of different phases depending on the growth kinetics, as well as tuning by interaction between the boron sheet and the substrate. This, however, remains an open question.

In this paper, we report two additional new phases of boron sheets on Ag(1 1 1), which, though relatively rarely observed, can be regularly reproduced in our experiment. The atomic structure and structural models of these two phases are systematically studied by scanning tunneling microscopy/spectroscopy

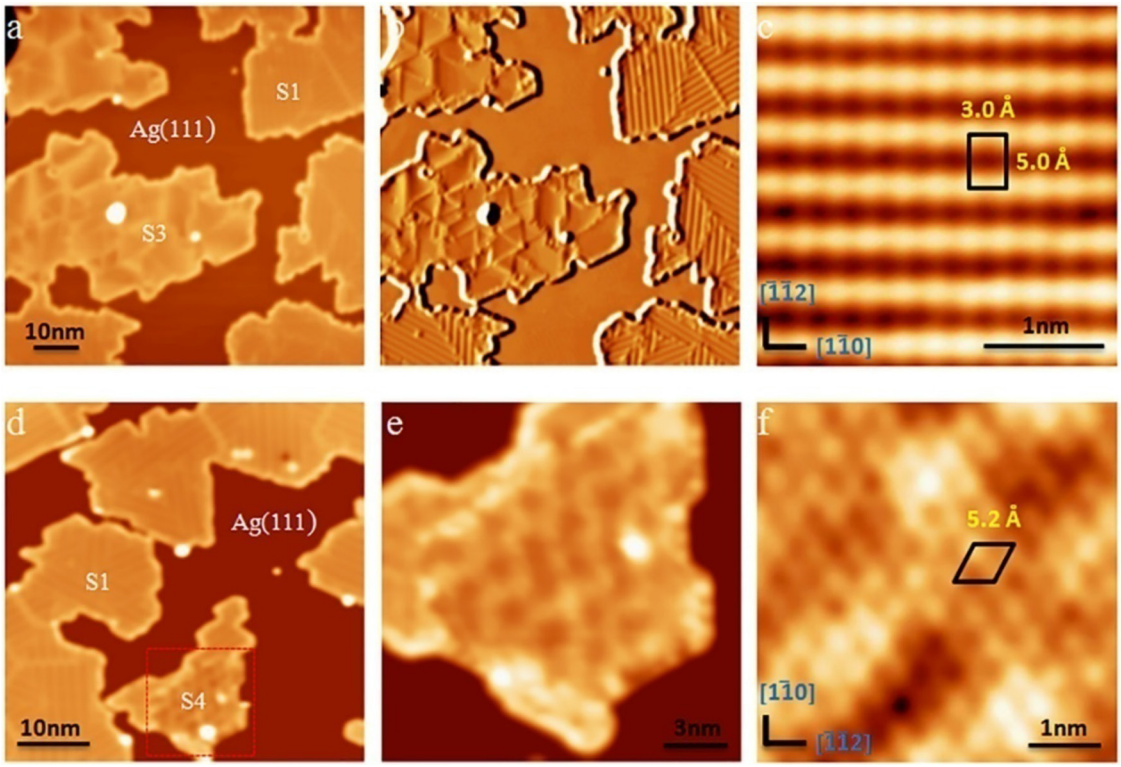

Figure 1. STM images of two metastable 2D boron sheets on Ag(1 1 1). (a) STM topographic image of boron structures on Ag(1 1 1). The boron islands are labelled as 'S1' and 'S3' phases. (b) The derivative STM image of (a). (c) High-resolution STM image of the S3 phases. The S3 unit cell is marked by a black rectangle. (d) STM topographic image of boron structures on Ag(1 1 1). The boron islands are labelled as 'S1' and 'S4' phases. Most boron islands shown in the image are S1 phase. (e) STM image obtained on the area marked by the red dotted rectangle in (d). (f) High-resolution STM image of the S4 phase. The S4 unit cell is marked by a black rhombus.

(STM/STS) and theoretical calculations. It turns out that one of the two phases, denoted as S3, shares the same atomic structure with S1 but has a different directional relationship with respect to the Ag(1 1 1) substrate. Meanwhile, the other new phase exhibits a hexagonal symmetry in its atomic structure, accompanied by moiré patterns due to the structure commensuration with the substrate. We suggest that this phase corresponds to the long-expected α-sheet. STS measurements indicate that both phases are metallic, similar to the previously reported S1 and S2 phases.

Boron sheets were grown on a single crystalline Ag(1 1 1) substrate in an ultra-high vacuum chamber (2.0×10^{-11} Torr) by direct evaporation of a pure boron source in an e-beam evaporator. A detailed preparation process can be found in our previous paper [19].The substrate was cleaned by several cycles of Ar^+ ion sputtering and annealing. The substrate was held at about 570 K during B deposition in a temperature window where the S1 (β_{12}) boron phase forms. After growth, the sample was *in situ* transferred to a connected vacuum chamber for characterization by STM/STS. All the STM characterizations were performed at 77 K.

Figure 1(a) is a typical STM image of the sample with about 0.8 monolayer (ML) boron coverage (1 ML refers to the atomic density of the β_{12} boron sheet). Monolayer boron islands several tens of nanometers in size are found to distribute uniformly on the surface. By carefully inspecting the atomic structure of these islands, we found that most of the islands are S1 phase, as reported previously by Feng *et al* [19]. However, one can regularly find some islands with an obviously different surface structure, denoted by S3. As shown in figure 1(a), the S1 islands in the right and bottom part of the image exhibit ordered stripes, while in the middle and top left of the image, two islands with an S3 phase feature a smooth surface and many bright domain boundary features. Figure 1(b) is the derivative STM image of figure 1(a), in which the significant differences between the S3 and S1 sheets are indicated. Statistical analysis shows that the percentage of the observed islands for the S1 sheet and S3 sheet is 92% and 8%, respectively. Figure 1(c) shows the high resolution STM image of the S3 phase. It turns out that it shares the same unit cell with the S1 boron sheet, having a rectangular crystal lattice of $a = 3.0$ Å and $b = 5.0$ Å. Compared with the S1 phase, the short side of the unit cell of the S3 phase is in the direction of [1 $\bar{1}$ 0] of Ag(1 1 1), while that of the S1 phase is in the [$\bar{1}$ $\bar{1}$ 2] direction of Ag(1 1 1). Therefore, the S3 sheet also very likely corresponds to the β_{12}-sheet in the literature [21], but with a rotation of the boron lattice of 30° relative to the Ag(1 1 1) substrate, as compared with the S1 sheets. The corresponding atomic structure model of the S3 sheet is shown in figure 2(a).

One of the characteristic features of the S1 sheet is the appearance of 1.5 nm-wide parallel stripes (as seen in figure 1(b)), which come from the commensuration between the β_{12} structural model and the lattice of the Ag(1 1 1) substrate in the [$\bar{1}$ $\bar{1}$ 2] direction [19]. In contrast, in the S3 sheet model, the lattice constant of the β_{12} boron sheet in the [$\bar{1}$ $\bar{1}$ 2] direction (the long side of the rectangle in figure 1(c))

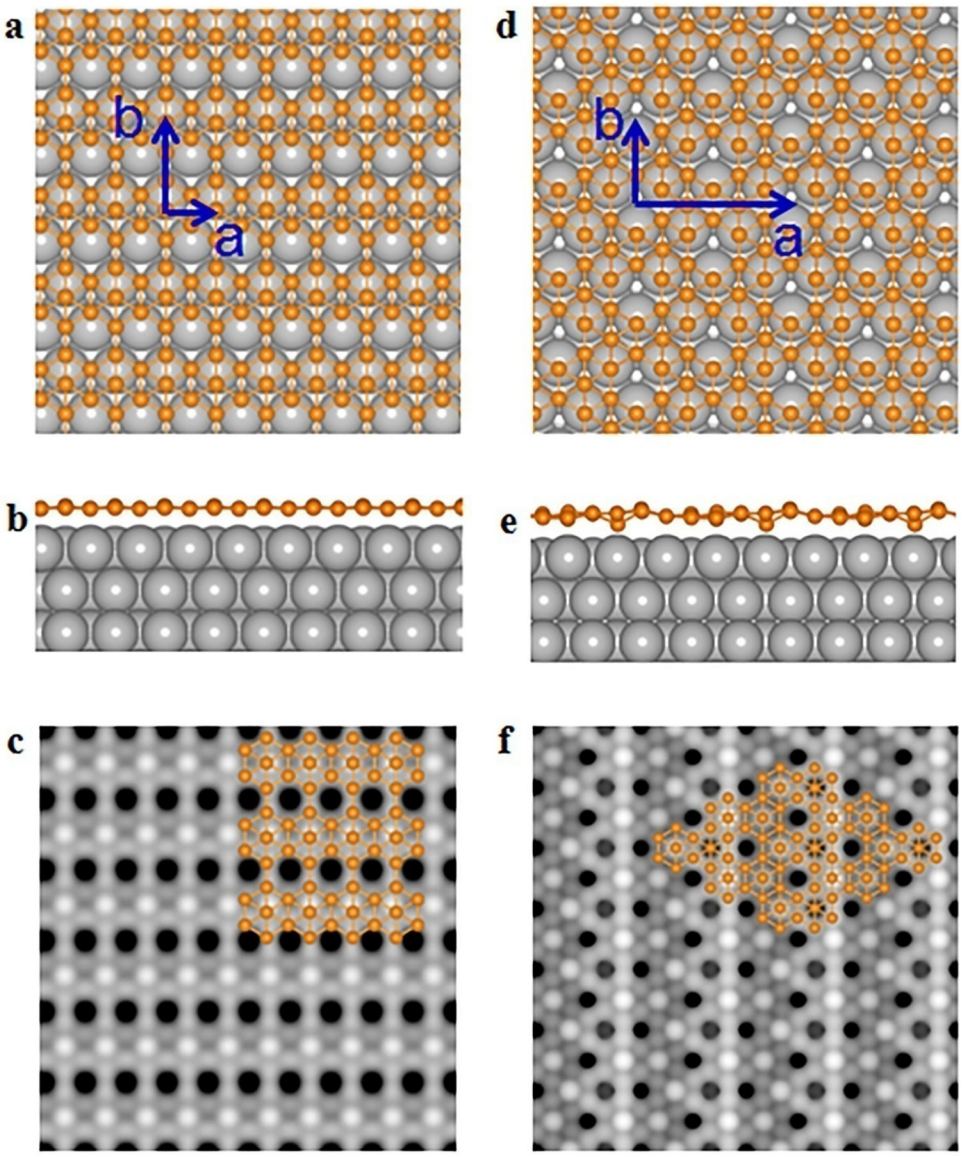

Figure 2. Structure models of the S3 and S4 phases of boron sheets based on DFT calculations. (a) and (b) Top and side views of the S3 model, which correspond to the β_{12} sheet of 2D boron on a Ag(1 1 1) surface. (c) Simulated STM topographic image of the β_{12} sheet. (d) and (e) Top and side views of the S4 model, which correspond to the α sheet of 2D boron on Ag(1 1 1). The α sheet was buckled by 1.1 Å in the z axis when put on Ag(1 1 1). (f) Simulated STM topographic image of the α sheet. The orange and grey balls in (a), (b), (d) and (e) represent boron and silver atoms, respectively. The basic vectors of the super cell, including the Ag(1 1 1) substrate, are marked by blue arrows. Models of the β_{12} and α sheets are superimposed on their simulated STM images.

(5.0 Å) matches very well with the period of Ag(1 1 1) (2.9 Å $\times \sqrt{3} = 5.02$ Å). Meanwhile, in the [1 $\bar{1}$ 0] direction (the short side of the rectangle in figure 1(c)), the lattice match is also very extraordinary (3.0 Å for S3 and 2.9 Å for Ag(1 1 1)). This perfect lattice matching corresponds perfectly with the experimental fact that no obvious moiré patterns should be observed in the S3 sheet.

The surface of the S3 sheet is very smooth in the STM images, as shown in figures 1(b) and (c). One characteristic feature observed on the S3 island surface is the appearance of bright lines, as shown in figures 1(a) and (b). High resolution STM images (not shown here) show that these bright lines are boundaries between the two S3 sheet domains; the detailed structure of these boundaries remains to be further investigated. In addition, from figure 1(b), it can be seen that the edge of the S3 islands is much brighter than the interior of the island. Such a bright edge should be due to a higher density of states at the edges of these boron sheets due to a charge accumulation in the edge, as we previously proposed for the S1 sheet [19]. More details on the edges of the S3 islands remain to be further investigated.

In addition, we observed another even more rarely observed, but regularly reproducible, new phase. As shown in figure 1(d) of another area of the same sample, most islands in this image are S1 islands, while there is a small island exhibiting a different structure, as denoted by the S4 phase. Figure 1(e) is the magnification of the dotted square region in figure 1(d), from which we observed that the S4 phase features are a bit irregular, but have clear hexagonal dark–bright moiré patterns. Note that the S4 island observed in our experiment is

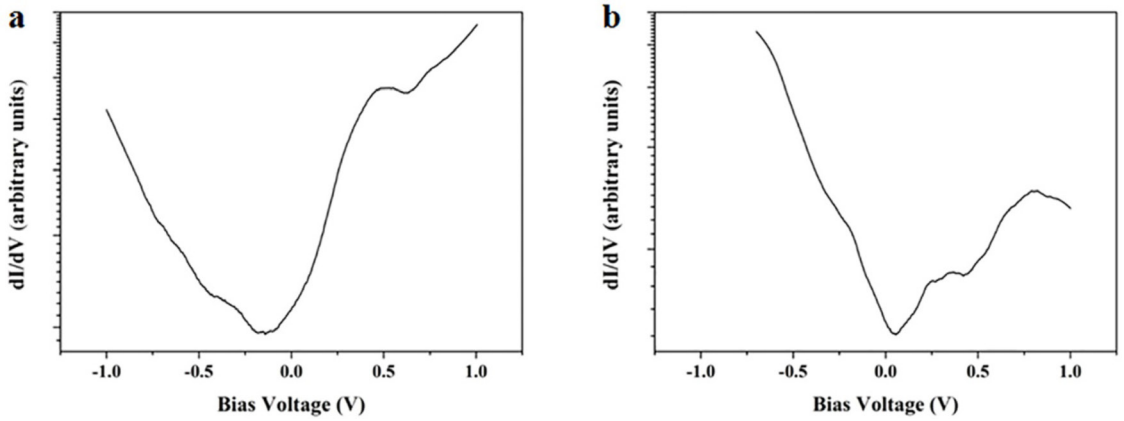

Figure 3. STS results for 2D boron sheets on Ag(1 1 1). (a) and (b) STS for S3 and S4 respectively. The voltage range of (a) is from −1 V–1 V. In (b), the voltage is from −0.7 V–1.0 V.

Table 1. Formation energies for free-standing and epitaxial S3 and S4 boron sheets. E_{FB} is the formation energy per atom for the free-standing boron sheet. E_{EB} is the formation energy per atom for the epitaxial boron sheet. ΔE is the adhesion energy of the boron sheet per boron atom.

	S3	S4
E_{FB}	6.23 (6.23)	6.27
E_{EB}	6.24 (6.32)	6.29
ΔE	0.01 (0.09)	0.02

commonly quite small. For example, in the marked S4 island in figure 1(d), only the inner part of the island exhibits a different structure, while the two edges of the island are still the S1 structure. Figure 1(f) shows the high resolution STM image of this phase. It has a hexagonal crystal lattice in addition to the global moiré pattern. The rhombic unit cell, as marked in figure 1(f), has a side length of 5.2 Å, which is very close to that of the long-expected α-sheet (5.0 Å).

In order to understand the structures of the S3 and S4 phases, we have carried out first principles calculations. DFT calculations were performed using a projector-augmented wave pseudopotential with the Perdew–Burke–Ernzerhof (PBE) function [25] and plane-wave basis set with an energy cut off at 400 eV. For the S3 phase, the calculation cell contained a boron film on a five-layer $1 \times \sqrt{3}$-Ag(1 1 1) surface. The surface Brillouin zone was sampled by a $13 \times 9 \times 1$ Monkhorst–Pack k-mesh. For the S4 phase, the boron film was positioned on a five-layer $3 \times \sqrt{3}$-Ag(1 1 1) surface. The Brillouin zone was sampled by a $5 \times 9 \times 1$ Monkhorst–Pack k-mesh. As the PBE function usually overestimates the chemical bond length, the lattice constant of Ag(1 1 1) used in the calculations was 3% larger than the experimental value, and a vacuum region of ~15 Å was applied. All the structures were fully relaxed until the force on each atom was less than 0.05 eV Å^{-1}, and the bottom two layers of silver atoms were fixed. Actually, in another DFT calculation, we also set the force criterion to 0.01 eV Å^{-1}, and the result was the same. The simulated STM images were obtained using the constant current mode based on calculated electron densities. All the calculations were performed with the Vienna *ab initio* simulation package [26]. Figures 2(a) and (b) display the proposed structure models of the S3 and S4 sheet on Ag(1 1 1), which correspond to the β_{12}-sheet and α-sheet, respectively. It is noted that the β_{12}-sheet retains its flat configuration on the Ag(1 1 1) surface, while the α-sheet spontaneously buckles by 1.1 Å in the z direction. Figures 2(e) and (f) are the simulated STM images of these two boron sheets on Ag(1 1 1), which are very close to that of the experimental STM images in figures 1(c) and (f). In the STM image (figure 1(d)), the S4 usually resides with the S1 phase. According to the atomic structure of boron sheets, the density of the hexagonal holes in S1 (1/6) is larger than S4 (1/9), which means that the β_{12} sheet (S1) is a little bit electron positive relative to the α-sheet (S4) [21]. From the view of electric neutrality, the fact that the S4 resides with the S1 phase may help in stabilizing the electron surplus in S4 on the Ag(1 1 1).

To figure out why we observe a much lower proportion of S3 and S4 phases on the surface compared to S1, we calculated the formation energy of these three structures and the results are shown in table 1. The formation energy of free-standing S3 was the same as S1, since they share the same structure. Nevertheless, the adhesion energy of S3 (0.01 eV per atom) on Ag(1 1 1) is smaller than that of S1 (0.09 eV per atom). Thus, the total formation energy for S3 (6.24 eV per atom) is smaller than that of S1 (6.32 eV per atom). This means that S3 is less energy favorable than S1 when adsorbed on Ag(1 1 1), resulting in the majority of the boron sheets being S1 phase. This situation was almost the same for S4, which has a formation energy of 0.03 eV per atom less than S1. It is noted that the formation of the four kinds of phases (including S1 and S2) is directly related to the substrate temperature during growth in our experiments. The S1, S3 and S4 phases are synthesized at a substrate temperature of 570 K, while the S2 is formed at 680 K. The boron flux was 0.001 ML s^{-1}. By using such a substrate temperature and boron flux, we can always find S1–S4 phases by searching on the surface, although the percentage of S3 and S4 phases are pretty small.

Theoretically, most 2D boron sheet structures proposed in the literature are metallic [11, 21–23, 27, 28], including the β_{12}-sheet and α-sheet. We have performed STS measurements for both the S3 and S4 phases. The results are shown in figure 3. The voltage range was from −1 V–1 V for S3

and −0.7 V–1 V for S4. To characterize possible energy gaps more accurately, the d*I*/d*V* axis was expressed in a logarithmic coordinate. The results indicate that both the S3 and S4 boron sheets are metallic, consistent with the theoretical predictions as well as the previous results on the S1 and S2 phases.

In conclusion, we have reported two new phases, namely S3 and S4 phases, of 2D boron sheets on a Ag(1 1 1) surface by MBE. We propose that the S3 is a β_{12}-sheet, the same as the previously reported S1 phase, but with a distinct rotational relationship with the Ag(1 1 1) substrate. On the other hand, the S4 sheet, which shows a clear hexagonal symmetry in contrast to all previously observed 2D boron phases, is proposed to be the long-expected α-sheet. STS measurements show that both the S3 and S4 phases are metallic, which agrees well with the theoretical predictions.

Acknowledgments

This work was supported by the MOST of China (grants nos. 2013CB921702, 2013CBA01601, 2016YFA0202301), the NSF of China (grants nos. 11334011, 11322431, 11304368, 11674366, 11674368), and the Strategic Priority Research Program of the Chinese Academy of Sciences (grant no. XDB07020100).

References

[1] Woods W G 1994 An introduction to boron: history, sources, uses, and chemistry *Environ. Health Perspect.* **102** 5
[2] Albert B and Hillebrecht H 2009 Boron: elementary challenge for experimenters and theoreticians *Angew. Chem., Int. Ed. Engl.* **48** 8640
[3] Ogitsu T, Schwegler E and Galli G 2013 β-Rhombohedral boron: at the crossroads of the chemistry of boron and the physics of frustration *Chem. Rev.* **113** 3425
[4] Szwacki N G, Sadrzadeh A and Yakobson B I 2007 B80 Fullerene: an *ab initio* prediction of geometry, stability, and electronic structure *Phys. Rev. Lett.* **98** 166804
[5] Kunstmann J and Quandt A 2006 Broad boron sheets and boron nanotubes: an *ab initio* study of structural, electronic, and mechanical properties *Phys. Rev.* B **74** 035413
[6] Singh A K, Sadrzadeh A and Yakobson B I 2008 Probing properties of boron α-tubes by *ab initio* calculations *Nano Lett.* **8** 1314
[7] Ciuparu D, Klie R F, Zhu Y and Pfefferle L 2004 Synthesis of pure boron single-wall nanotubes *J. Phys. Chem.* B **108** 3967
[8] Wang X, Tian J, Yang T, Bao L, Hui C, Liu F, Shen C, Gu C, Xu N and Gao H 2007 Single crystalline boron nanocones: electric transport and field emission properties *Adv. Mater.* **19** 4480
[9] Liu F, Shen C, Su Z, Ding X, Deng S, Chen J, Xu N and Gao H 2010 Metal-like single crystalline boron nanotubes: synthesis and *in situ* study on electric transport and field emission properties *J. Mater. Chem.* **20** 2197
[10] Zhai H *et al* 2014 Observation of an all-boron fullerene *Nat. Chem.* **6** 727
[11] Tang H and Ismail-Beigi S 2007 Novel precursors for boron nanotubes: the competition of two-center and three-center bonding in boron sheets *Phys. Rev. Lett.* **99** 115501
[12] Liu H, Gao J and Zhao J 2013 From boron cluster to two-dimensional boron sheet on Cu(1 1 1) surface: growth mechanism and hole formation *Sci. Rep.* **3** 3238
[13] Liu Y, Penev E S and Yakobson B I 2013 Probing the synthesis of two-dimensional boron by first-principles computations *Angew. Chem., Int. Ed. Engl.* **52** 3156
[14] Zhang Z, Yao Y, Gao G and Yakobson B I 2015 Two-dimensional boron monolayers mediated by metal substrates *Angew. Chem., Int. Ed. Engl.* **54** 13022
[15] Xu S, Zhao Y, Liao J, Yang X and Xu H 2016 The formation of boron sheet at the Ag(1 1 1) surface: from clusters, ribbons, to monolayers in preparation (arXiv:1601.01393)
[16] Castro Neto A H, Guinea F, Peres N M R, Novoselov K S and Geim A K 2009 The electronic properties of graphene *Rev. Mod. Phys.* **81** 109
[17] Geim A K and Novoselov K S 2007 The rise of graphene *Nat. Mater.* **6** 183
[18] Mannix A J *et al* 2015 Synthesis of borophenes: anisotropic, two-dimensional boron polymorphs *Science* **350** 1513
[19] Feng B, Zhang J, Zhong Q, Li W, Li S, Li H, Cheng P, Meng S, Chen L and Wu K 2016 Experimental realization of two-dimensional boron sheets *Nat. Chem.* **8** 563
[20] Tao L, Cinquanta E, Chiappe D, Grazianetti C, Fanciulli M, Dubey M, Molle A and Akinwande D 2015 Silicene field-effect transistor operating at room temperature *Nat. Nanotech.* **10** 227
[21] Wu X, Dai J, Zhao Y, Zhuo Z, Yang J and Zeng X 2012 Two-dimensional boron monolayer sheets *ACS Nano* **6** 7443
[22] Penev E S, Bhowmick S, Sadrzadeh A and Yakobson B I 2012 Polymorphism of two-dimensional boron *Nano Lett.* **12** 2441
[23] Zhang Z, Penev E S and Yakobson B I 2016 Two-dimensional materials: polyphony in B flat *Nat. Chem.* **8** 525
[24] Zhang Z, Mannix A J, Hu Z, Kiraly B, Guisinger N P, Hersam M C and Yakobson B I 2016 Substrate-induced nanoscale undulations of borophene on silver *Nano Lett.* **16** 6622
[25] Perdew J P, Burke K and Ernzerhof M 1996 Generalized gradient approximation made simple *Phys. Rev. Lett.* **77** 3865
[26] Kresse G and Furthmüller J 1996 Efficient iterative schemes for *ab initio* total-energy calculations using a plane-wave basis set *Phys. Rev.* B **54** 11169
[27] Tang H and Ismail-Beigi S 2009 Self-doping in boron sheets from first principles: a route to structural design of metal boride nanostructures *Phys. Rev.* B **80** 134113
[28] Ozdogan C, Mukhopadhyay S, Hayami W, Guvenc Z B, Pandey R and Boustani I 2010 The unusually stable B100 fullerene, structural transitions in boron nanostructures, and a comparative study of α- and γ-boron and sheets *J. Phys. Chem.* C **114** 4362